

# On Computational Complexity of 3D Ising Spin Glass: Lessons from D-Wave Annealer

Hao Zhang<sup>1</sup> and Alex Kamenev<sup>1,2</sup>

<sup>1</sup>*School of Physics and Astronomy, University of Minnesota, Minneapolis, MN 55455, USA and*

<sup>2</sup>*William I. Fine Theoretical Physics Institute, University of Minnesota, Minneapolis, MN 55455, USA*

Finding an exact ground state of a 3D Ising spin glass is proven to be an NP-hard problem [1]. Given validity of the exponential time hypothesis [2], its computational complexity was proven to be no less than  $2^{N^{2/3}}$  [3], where  $N$  is the total number of spins. Here we report results of extensive experimentation with D-Wave 3D annealer with  $N \leq 5627$ . We found exact ground states (in a probabilistic sense) for typical realizations of 3D spin glasses with the efficiency, which scales as  $2^{N/\beta}$  with  $\beta \approx 10^3$ . Based on statistical analysis of low energy states, we argue that with an improvement of annealing protocols and device noise reduction,  $\beta$  can be increased even further. This suggests that, for  $N < \beta^3$ , annealing devices provide a most efficient way to find the ground state.

## I. INTRODUCTION

Optimization problems are ubiquitous across science, technology, and industry [4, 5]. A large class of such problems can be formulated as a task of finding a bit-string,  $\{\sigma^z\} = \{\pm 1, \pm 1, \dots, \pm 1\}$ , of length  $N$ , which minimizes a certain cost function,  $H[\{\sigma^z\}]$ . While the latter can, in principle, assume an arbitrarily complicated form, many studies [6–16] restrict it to a quadratic form, which mimics binary interactions of Ising spins:

$$H[\{\sigma^z\}] = \sum_{i < j} J_{ij} \sigma_i^z \sigma_j^z. \quad (1)$$

Here an  $N \times N$  matrix  $J_{ij}$  encodes coupling strengths between the spins. A physically and conceptually important example is provided by the Edwards-Anderson (EA) model of a spin glass [11, 17–21], where  $J_{ij}$ 's are restricted to a lattice in  $D$  spatial dimensions, and are randomly and independently drawn from a distribution with zero mean and width  $J$ . Hereafter we put  $J = 1$  and thus measure the energy (i.e. the cost function) in this dimensionless unit.

It was proven [1, 22, 23] that finding a spin configuration, out of  $2^N$  possibilities, exactly minimizing the EA energy in  $D > 2$  is an NP-hard problem [24, 25]. This means that no known algorithm (classical or quantum) [21, 26–56] can find, or verify an answer in a polynomial time. For  $D = 3$  it was proven [3] that no algorithm can be more efficient than  $2^{N^{2/3}}$  in the  $N \rightarrow \infty$  limit, provided *exponential time hypothesis* (ETH) [2] holds. We provide a simple illustration of  $N^{2/3}$  algorithm in section V. These results do not limit the possibility of an algorithm (or an analog device) with the exponential scaling,  $\sim 2^{N/\beta}$ , which is more efficient for  $N < \beta^3$ . Here  $\beta$  is a constant specific to a given hardware and software implementation of a computation procedure [57, 58]. The goal of this paper is to discuss if there are fundamental physical limits on  $\beta$ , based on extensive experimentation with the D-Wave 3D annealer [49–56].

Despite its 50-year history, the physics of the 3D EA model is not yet fully understood. The debate [59–70] is between the replica symmetry breaking (RSB) scenario

and the droplet picture. The RSB expects (exponentially) many local minima, which are  $O(1)$  close in energy and  $O(N)$  in Hamming distance away from each other – the so-called *non-trivial* ground state. The droplet picture predicts a unique (aka *trivial*) ground state. Local minima, which are Hamming distance  $L$  away from the ground state, have an excess energy which scales as  $L^{\tilde{\theta}}$  with  $\tilde{\theta} > 0$ . There are also intermediate *trivial-non-trivial* (TNT) scenarios [62, 71, 72], which combine between the two.

Our data support a sort of TNT picture with a unique ground state and non-trivial low-energy excitations. Specifically, we found that the number of local minima (or rather *basins* of attraction, defined below) with the excess energy  $\delta = E - E_0$ , separated by a Hamming distance of order  $N$ , scales as

$$m(\delta, N) \propto \exp\left(\frac{\delta}{2\delta_0}\right). \quad (2)$$

Here  $E$  is an energy of a deep minimum;  $E_0$  is the ground state energy; and  $\delta_0 = -E_0/N > 0$  is the ground state energy per spin (for the D-Wave Advantage architecture,  $\delta_0 \approx 1.6$ ). Therefore for the excess energy  $\delta \sim O(1)$ , there are  $O(1)$  distant basins, suggesting (almost) unique ground state. On the other hand, the number of such distant basins proliferates exponentially for  $\delta \gg 1$ , pointing to a very small or zero exponent  $\tilde{\theta}$ .

Using the D-Wave annealer and the cyclic annealing protocol [73, 74] we generate a large ensemble of low-energy states. Their average excess energy,  $\delta$ , appears to scale linearly with the system size,  $N$ ,

$$\delta \approx N/\beta_{\text{eff}}, \quad (3)$$

where  $1/\beta_{\text{eff}}$  – the average excess energy per spin, may be loosely identified with an effective temperature of the generated ensemble. We then show that, given sufficiently many states per basin (in practice their number scales as  $N$ ), one can digitally “cool” the ensemble down to the true ground state (with a probability which may be consistently increased by increasing the size of the ensemble of states).

The computational effort involved in this procedure thus scales as  $Nm(\delta, N) \propto e^{N/(2\delta_0\beta_{\text{eff}})}$ , focusing on the

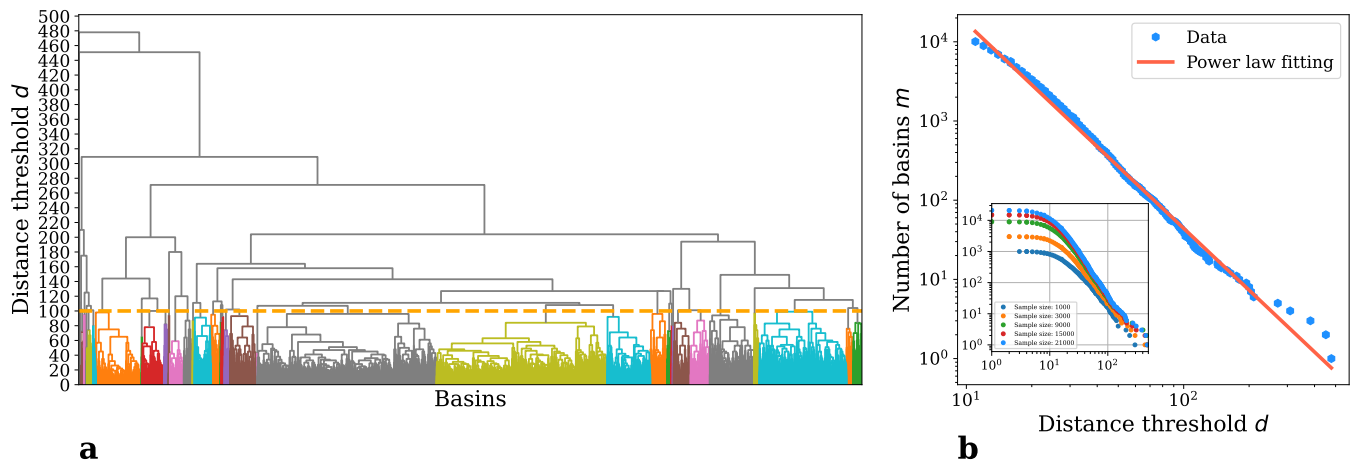


FIG. 1: (a) A dendrogram illustrating the hierarchical clustering of basins, based on a set of 21000 low-energy states within a small energy window for a system with  $N = 958$ . Orange dashed line indicates basins counting at  $d = 100$ . (b) Relationship between the distance threshold,  $d$ , and the number of basins  $m$ , fitted with a power law (red line). The inset shows convergence of the observed number of basins as the number of low-energy states increases.

exponent. This leads to  $\beta = (2\delta_0 \log 2)\beta_{\text{eff}} \approx 2.2\beta_{\text{eff}}$ . Therefore the computational complexity is tight to the inverse effective temperature,  $\beta_{\text{eff}}$ , of an available sufficiently large ensemble of low-energy states. The D-Wave annealer and cyclic annealing allows us to reach  $\beta_{\text{eff}}$  in excess of  $10^3$  in  $10\text{ ms}$  time per one low-energy state.

It is worth noting that exact numerical algorithms for 3D EA model, such as branch-and-cut [4], have been reported [57] to reach the efficiency of  $\beta \approx 10^2$  for typical instances. Analog devices, such as D-Wave, can apparently increase it by at least another order of magnitude (admittedly, in a probabilistic rather than in the exact sense). It is likely that the effective temperature can be reduced even further.

How low can the effective temperature [75],  $1/\beta_{\text{eff}}$ , be? Empirically, we found that

$$\beta_{\text{eff}} \approx 560 \left( \frac{\tau}{20 \mu\text{s}} \right)^{0.16}, \quad (4)$$

in the available range  $2 \mu\text{s} < \tau < 2\text{ ms}$ , where  $\tau$  is the annealing time per cycle. Note that this entire range is far from the adiabatic regime, even for our smallest systems with  $N$  around 500. The annealing was always performed in the non-adiabatic regime [76]. Yet, the cyclic annealing is capable of “cooling” the system down to a very low effective temperature of  $10^{-3}$ . We expect that the temperature decrease with the increasing annealing time will saturate at a sufficiently large  $\tau$  (though we could not confirm it experimentally due to imposed limits). If there are no fundamental limitations on how long such saturation time can be, it seems plausible that  $\beta_{\text{eff}}$  can be further increased with an improved hardware and annealing protocols [77]. We thus conjecture that there is no fundamental limit on  $\beta$ . The situation is reminiscent of the third law of thermodynamics, which precludes reach-

ing zero temperature but does not place limitations on how low the temperature can be.

The rest of the paper is organized as follows: in Section II we present our results for the number of low-energy states and basins in 3D EA spin glasses. Section III is devoted to the digital “cooling” post-processing algorithm. In Section IV, we describe our results for a set of large size spin glasses. Section V provides a short summary and discussion of the key ingredients of our conclusions.

## II. BASINS AND COUNTING FORMULA

We implemented 3D spin glasses with the Hamiltonian given by Eq. (1) on D-Wave’s Advantage 4.1 quantum processor, where  $J_{i<j}$ ’s are independently drawn from the uniform distribution over the interval  $[-1, 1]$ . The Pegasus architecture [78], denoted  $P_M$ , was used for various system sizes. This architecture is a 3D cubic lattice  $(M-1) \times (M-1) \times 12$ , with two spins per unit cell. The data presented in this section was generated using standard forward annealing protocol.

In spin glasses, a basin represents a set of states with similar energies and Hamming distances between any two of them below a certain threshold, denoted as  $d$ . To visualize and organize the basins, we used dendrograms, see Fig. 1a. The horizontal axes here labels 21,000 low-energy states collected for a system size  $N = 958$  within a specific narrow energy window. We employed the complete linkage method from SciPy library [79] to generate basins. Each horizontal line in the dendrogram represents a distance threshold,  $d$ ; all states connected to it form a basin with the threshold  $d$ . Figure 1b, shows the number of basins  $m(d)$  at a given distance  $d$ , i.e. a number of vertical lines intersected by a horizontal line (e.g. the orange dashed line in Fig. 1a at a height  $d$ ). One observes

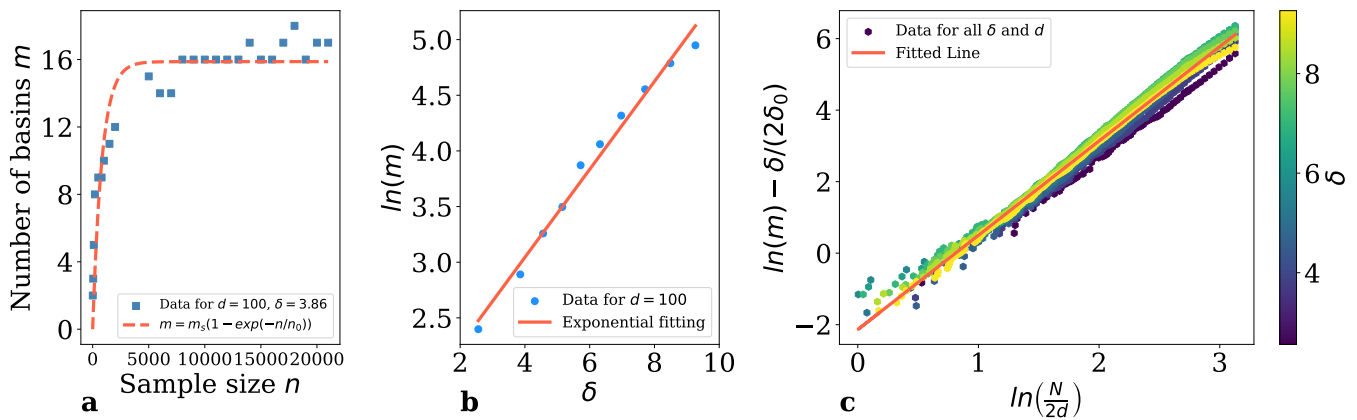


FIG. 2: (a) Number of observed basins as a function of a number,  $n$ , of low energy states used for the dendrogram;  $d = 100$  and  $\delta = 3.86$ . The dashed red line is a fit to  $m = m_s[1 - \exp(-n/n_0)]$ , where  $m_s$  is given by Eq. (6) and  $n_0 = 1600$ . (b) Exponential relationship between  $\ln(m)$  and  $\delta = E - E_0$ . The red line represents the exponential fit. (c) Data collapse on Eq. (6) for all values of  $\delta$  and  $d$  when plotting  $\ln(m) - \delta/(2\delta_0)$  versus  $\ln(N/2d)$ . Color of data points encodes values of  $\delta$ , as shown on the right.

that  $m(d)$  follows a power law scaling:

$$m(d) = C \left( \frac{N}{2d} \right)^\alpha, \quad (5)$$

where the fitting parameters are  $\alpha \approx 2.6$  and  $C \approx 0.76$ . Below we show that  $C$  is very sensitive to the specific energy window, while  $\alpha$  is practically energy-independent. One may worry that Eq. (5) is a property of a number of collected states. The inset in Fig. 1b, shows that adding more states within the same energy window adds extra basins at smallest  $d$ 's, while larger  $d$ 's quickly saturate to the relation (5), see Fig. 2a [80].

To investigate the energy dependence of Eq. (5), we generated ten groups of states that ranged from the lowest to a relatively high energy. Each group has 21,000 states within a specific small energy window. We then construct the dendrograms and repeat the counting procedure, described above. The results are presented in Figs. 2b,c and are summarized with the best fit:

$$m(\delta, d) = C_0 \exp \left\{ \frac{\delta}{2\delta_0} \right\} \left( \frac{N}{2d} \right)^\alpha. \quad (6)$$

Here  $\delta = E - E_0$ , where  $E$  is the center of the energy window and  $E_0$  is the ground state energy (a way we determine  $E_0$  is discussed below),  $\delta_0 = |E_0|/N \approx 1.6$ , and  $C_0 \approx 0.08$ .

Focusing on the lowest energies,  $\delta \sim O(1)$ , one may ask to how many distant,  $d \sim O(N)$ , basins do such low-energy states belong? According to Eq. (6) the typical answer is *one*. There is typically a *single* basin, which contains both the ground state and all (or most) of low-energy excited states within the energy window  $E_0 < E < E_0 + 1$ . This observation seems to support the droplet picture[59–61, 69]. On the other hand, both the total number of states and the number of distant basins, they belong to, grow exponentially once  $E - E_0 \gg \delta_0$ .

The proliferation of the number of distant basins for different energy levels above the the ground state is illustrated schematically in Fig. (3).

### III. DIGITAL COOLING TECHNIQUE

As we have seen in the previous section, the number of distant basins grows exponentially with energy. Yet, if  $\delta$  is not too large there is still a finite number of them. Suppose this is the case and one can generate sufficiently many low-energy states to cover *all* the distant basins

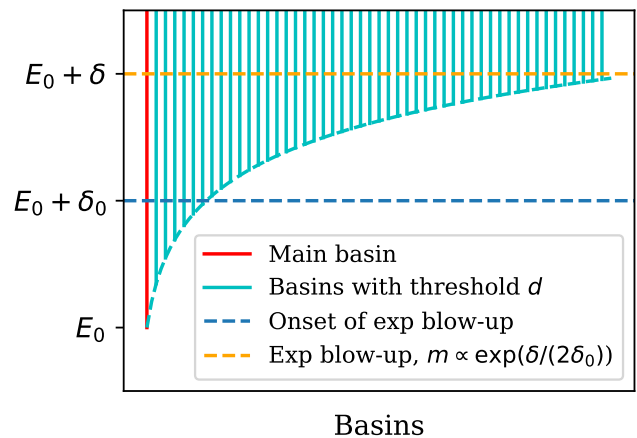


FIG. 3: Schematic illustration for proliferation of distant basins. The main basin (in red) corresponds to the region near the exact ground state, which has energy  $E_0$ . As the energy increases, basins (in cyan) proliferate. Dashed lines illustrate number of basins at each energy level  $E = E_0 + \delta$ .

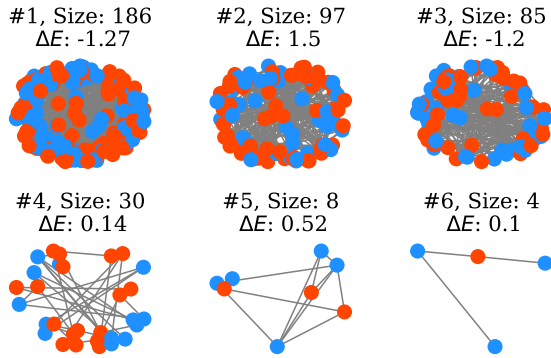


FIG. 4: Examples of connected clusters with small surface energy between two low-energy states with a total Hamming distance about 450. Six largest clusters are shown here. Blue nodes denote up-spin while red nodes denote down-spin.

and moreover have sufficiently many states falling within each big basin. We show that this is sufficient to recover the true ground state.

The core idea is based on the fact that each basin in the spin glass landscape has an ancestor – a state with lowest energy, from which all other states are generated. Similar to the droplet picture, all the excited states are results of flipping a number of relatively limited porous clusters (or droplets) of spins with a small surface energy. The idea thus is to identify such loosely connected clusters within each basin. By selectively flipping individual clusters one can proceed lowering the energy until the bottom of the basin is reached. The procedure, outlined below, directs the process towards the single deepest basin and thus converges to the true ground state.

To identify such clusters, we calculate a Hamming distance,  $d$ , between a pair of low-energy states. This implies that  $d$  spins should be flipped to go from one of those states to the other. We now focus on those  $d$  spins, which are different between the two states, and look if they are connected on the lattice through non-zero  $J_{ij}$  couplings. This splits the  $d$  spins into a several connected clusters, which do not have any non-zero couplings between each other. Examples of such clusters with their sizes and surface (i.e. flip-) energies are illustrated in Fig. 4, while a statistical analysis of these characteristics was done in Ref. [74]. Notice that, despite large sizes of some of these clusters, the energy change of flipping the entire cluster is rather small,  $O(1)$ . Such clusters may be digitally flipped independently from each other to generate new low-energy states.

The digital cooling technique works as follows: consider a set of low-energy states produced by the annealer. Pick one state and compare it pairwise, as discussed above, with all other states within the set. This identifies a library of clusters, which may be flipped in the

picked state resulting in small energy changes. Choose now one such cluster, which promises largest energy decrease and flip it in the picked state. This generates a parent state with a lower energy than the originally picked one. Repeat this procedure for all the states in the set and produce parents for each one of them. Some of these parents may happen to coincide, meaning that their original states are excitations (i.e. cluster flips) of the same ancestor. Repeat the same procedure for the set of parent states to produce the generation of grand-parents, then grand-grand-parents, etc. Number of ancestors keeps decreasing in every step of this process, due to a frequent coalescence of them. In practice, in a very few generations all the ancestors collapse to a one single state – a common ancestor, and thus the process stops. A similar procedure was developed in Refs. [42–44].

The procedure guarantees that each deeper generation has energies smaller than their kids. According to Eq. (6) and Fig. 3, this implies fewer basins available for such lower energy set of states. As a result, Fig. 3 works like a sink, which directs the algorithm towards the unique ground state. Given a sufficiently large initial set, the common ancestor state must be the ground state.

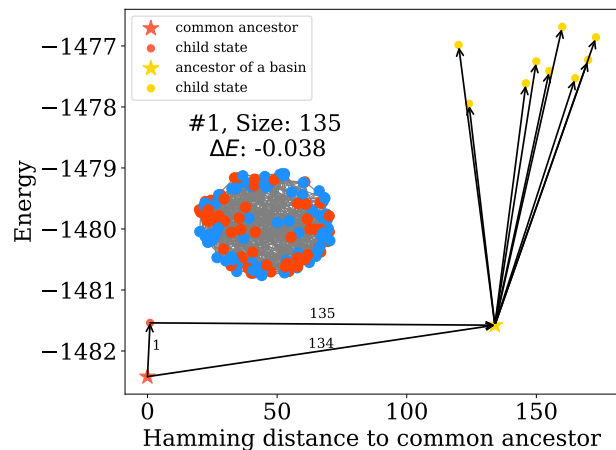


FIG. 5: Illustration of the exact ground state acting as a common ancestor (red star). A distant ancestor (yellow star) is generated from the common ancestor by flipping a 134-size cluster or equivalently by flipping a single spin first to a child state (red dot) and then flipping a 135-size nearly-zero-energy cluster (shown in inset). States in a basin (yellow dots) are generated from the ancestor (yellow star) through some small-size clusters flipping.

Figure 5 illustrates an example of such genealogy tree, which may be reconstructed with the cluster flipping procedure. The larger clusters play a special role by moving the common ancestry search from one distant basin to another. The exact ground state is the common ancestor of all states. An offspring ancestor is generated from the common ancestor by flipping a large cluster with a

small energy. In Fig. 5 a higher-energy state is generated by flipping a specific spin in the common ancestor. Then, the offspring ancestor in the right part is generated by flipping a cluster of size 135 and energy  $-0.038$ . All states in the ancestor's basin or higher-energy basins in the same pillar can now be generated through small cluster flips from the ancestor. In practice, the ancestry search runs in the opposite direction: from top to the bottom.

#### IV. FINDING GROUND STATES OF LARGE SPIN GLASSES

To illustrate the procedure we discuss its details for 3D spin glass systems of sizes  $N = 958$  and  $N = 5627$ . It starts from running the cyclic annealing [73] with random initial states to generate a large ergodic ensemble of low-energy states. Implementation details can be found in Ref. [74]. This approach reaches notably deeper energy levels compared to the forward annealing. After collecting sufficiently many of such states, we randomly divide them into smaller groups and run the digital cooling (ancestry search) algorithm within each group.

In the case of  $N = 958$ , we repeatedly found *exactly* the same common ancestor state in each of independently generated groups. Fig. 6a shows the data for a random typical realization of the glass; 500 low-energy states (denoted by blue lines) were generated and divided into 25 groups, each containing 20 states. Each group corresponds to a column in the figure, and the common ancestor state from each group (after digital cooling) is marked with a red line. All 25 groups produced *exactly* the same state, with the energy  $-1482.421$ . We believe that the probability this state is *not* the true ground state approaches zero exponentially with the number of groups, yielding the same ancestor. This scenario was consistently reproduced in several random realizations of  $N = 958$  EA spin glasses.

In case of  $N = 5627$  we generated 4000 low-energy states through the cycle annealing with random initial states. Those states were randomly split into 80 groups of 50 states each, blue lines in Fig. 6b. After applying the digital cooling, a common ancestor for each group was generated. In this case most of these common ancestors do not coincide, orange lines in Fig. 6b. Their energies form a distribution centered at about  $-8958$  with the standard deviation,  $\sigma_1 = 1.16$  (to compare the initial (blue) states were centered at  $-8944$  with the standard deviation  $\sigma_0 = 4.39$ ).

We then divide a set of 80 common ancestor states into 2 second-generation groups. After applying digital cooling to each of these two groups, we found them yielding two very close (yet still different by a single cluster of 67 spins) common ancestors with extremely close energies  $-8961.40$  and  $-8961.11$ , red lines in Fig. 6b. We believe the first one is the true ground state, though the confidence level of this assertion is much less than for

$N = 958$ .

To investigate dependence of the computational complexity on the system size, we kept the cyclic quantum annealing settings fixed (same annealing time, protocol, and number of cycles) and tested system sizes,  $N = 678, 958, 1312, 2084, 5627$ . The cycle annealing with random initial conditions produces a narrow Gaussian-like distribution of energies. Figure 6c shows that both the average residual energy,  $\delta/2\delta_0$ , and the standard deviation,  $\sigma$ , scale approximately linearly with the system size,  $N$ , with slopes of  $10^{-3}$ , Eq. (3), and  $2.6 \times 10^{-4}$ , correspondingly. To know the absolute scale of the excess energy, one needs to know the ground state energy for each system size. The digital cooling algorithm was run for each system size. Except for the largest case of  $N = 5627$ , it rapidly converges to an exactly same common ancestor. Its energy was taken as,  $E_0$ .

The linear relationship (3) may be interpreted as a finite density per volume of disconnected clusters with a smooth distribution of  $O(1)$  energies. The number of excited (flipped) clusters per unit volume is dictated by an inherent noise of the non-adiabatic annealing process. The magnitude of such noise, and thus  $\beta_{\text{eff}}$  in Eq. (3), may be controlled by changing the annealing rate. Figure 6d shows  $\beta_{\text{eff}}$  as a function of the annealing time per cycle,  $\tau$ , with the fit given by Eq. (4).

#### V. DISCUSSION AND CONCLUSION

For completeness let us discuss here an algorithm producing a sub-exponential complexity,  $\sim 2^{4N^{2/3}}$  [81]. Consider a cube of size  $L = N^{1/3}$  and let's assume that its ground state can be found with a complexity  $2^{f(L)}$ . Let us now slice this cube in three orthogonal directions onto 8 cubes of size  $L/2$ . Given a fixed configuration of spins sitting on the three cutting planes, the 8 cubes are completely *uncoupled* thanks for the nearest neighbor interactions of the EA model. Therefore for every of  $2^{3L^2}$  configurations of the spins on the cutting planes, one needs to determine a ground state for each of 8 cubes of size  $L/2$  independently. To this end we will cut each of  $L/2$  cubes into 8 cubes of size  $L/4$ , etc. Complexity of this procedure is thus  $2^{3L^2} \times 8 \times 2^{f(L/2)}$ , which leads to the recursion relation

$$f(L) = 3L^2 + 3 + f(L/2). \quad (7)$$

Easy to see that it is solved with  $f(L) = 4L^2 + 3 \log_2 L$ , resulting in the complexity  $N \times 2^{4N^{2/3}}$ . It is possible that with a smarter bookkeeping the factor of 4 in the exponent can be somewhat reduced. However, it can not be less than 1, according to the lower bound on the complexity, proven in Ref. [3], under the assumption of ETH [2] validity. Our point here is to demonstrate an existence of a sub-exponential,  $N^{2/3}$ , algorithm.

Based on the data obtained with the D-Wave Advantage annealer, we observed an exponential scaling,  $2^{N/\beta}$ ,

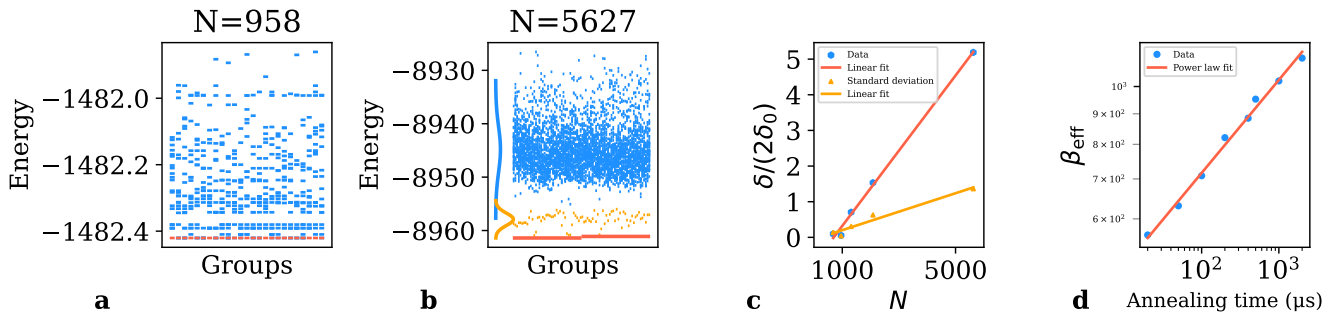


FIG. 6: (a) For  $N = 958$ , 500 low-energy states (blue lines) are divided into 25 groups. Common ancestor states, generated through the digital cooling, are shown by red lines. They are the same for all 25 groups, with the energy  $-1482.421$ . (b) For  $N = 5627$ , 4000 low-energy states (blue lines) are divided into 80 groups. The orange lines represent common ancestors in each group. Curves on the left show the energy distributions before and after digital cooling. The orange states were divided into two groups, yielding two very close common ancestors (red lines). (c) Average energy  $\delta/(2\delta_0)$  (blue dots) and standard deviation,  $\sigma$  (orange dots) as functions of the system size,  $N$ , for a fixed cyclic quantum annealing protocol. The linear fit (red),  $\delta/(2\delta_0) = 0.00105N - 0.733$ . (d) The inverse average residual energy per spin,  $\beta_{\text{eff}}$ , as a function of the annealing time per annealing cycle. All other parameters are fixed. A power law relation (4) is found by the linear fit of the log-log plot.

which is, of course, inferior in the limit  $N \rightarrow \infty$ . Yet, we found  $\beta \approx 10^3$ , and argued that it is feasible to increase it even further. This implies that for  $N < \beta^3$ , the annealer with its exponential scaling is more efficient than the sub-exponential algorithm. (For  $N > \beta^3$ , the sub-exponential method requires a computational time in excess of  $2^{\beta^2}$ , which is not viable even for  $\beta = 10$ .)

The venue to reach a very large  $\beta$  is not universal across optimization tasks, or even spin-glass models. There are reasons to believe that it is restricted to short-range, spatially local models (so is the sub-exponential algorithm, as well). Indeed, the three ingredients are proven to be crucial for reaching large values of  $\beta$ : (i) basins counting formula, Eq. (6), which predicts a finite number of distant basins in a window  $O(1)$  above the ground state and its exponential growth with the energy; (ii) linearity with  $N$  of the residual energy, reachable with the annealer, Eq. (3); (iii) availability of the digital cooling, allowing one to reach the true ground state, given sufficiently many low-energy states per basin are available.

All these three ingredients are heavily predicated on (and provide a strong support to) some variant of droplet, or TNT picture. They all are based on the idea of independent, relatively small, disconnected from each other excitation clusters. None of them holds for the all-to-all Sherrington-Kirkpatrick (SK) model, or even within RSB picture of 3D spin glass. The number of distant basins there is exponential down to the  $O(1)$  energy, there is no reason why the residual energy should scale linearly with the system size, and digital cooling does not work, since any two states are always connected by one single giant cluster. It is probably by these reasons, that no large  $\beta$  was reported for SK model. The largest, we are

aware of, is  $\beta = 1/0.226 = 4.42$ , recently proved for a quantum algorithm [82]. While it is possible that it will be somewhat increased, one may expect that there is a fundamental limit on it.

Finally we address an issue of whether the quantum nature of the annealer is important for these conclusions. In our opinion it is *not*. Both classical and quantum annealing can, in principle, reach a low average residual energy per spin,  $1/\beta_{\text{eff}}$ , Eq. (3). One may argue that low effective temperature requires reduction of the internal noise and thus reduction of the physical temperature, where the quantumness inevitably shows up. It is thus plausible that quantum devices are capable of reaching larger  $\beta$ 's than classical ones. On the other hand, one may think of a “quantum-inspired” algorithms, e.g., where coupled spins evolve in transverse fields according to the classical Landau-Lifshitz-Gilbert equation [83]. To the best of our understanding, it is not clear if such fully classical algorithm is inherently inferior to the non-adiabatic quantum annealing.

Several open questions remain. One key question is how to improve  $\beta_{\text{eff}}$  in practice, whether through advancements in cyclic quantum annealing [73, 74], improvements in quantum devices [55], or the implementation of exotic quantum drivers [84]. Another open question is whether particularly hard instances exist beyond random realizations for large spin glasses.

## VI. ACKNOWLEDGMENTS

We are grateful to Mohammad Amin, Dmitry Bagrets, Andrew Berkley, Emile Hoskinson, David Huse, Liang Jiang, Andrew King, Giorgio Parisi, Jack Raymond,

Boris Shklovskii, and Michael Winer for insightful discussions. This work was supported by the NSF grant DMR 2338819.

<https://doi.org/10.5281/zenodo.14578166>. Additional data analyzed in this study can be obtained from the corresponding author upon request.

## VII. DATA AVAILABILITY

The realizations and their ground states for spin glasses of various sizes are available via the following link:

- 
- [1] F. Barahona, On the computational complexity of ising spin glass models, *Journal of Physics A: Mathematical and General* **15**, 3241.
- [2] R. Impagliazzo and R. Paturi, Complexity of k-sat, in *Proceedings. Fourteenth Annual IEEE Conference on Computational Complexity (Formerly: Structure in Complexity Theory Conference) (Cat.No.99CB36317)* (1999) pp. 237–240.
- [3] Z. Zhang, Computational complexity of spin-glass three-dimensional (3d) ising model, *Journal of Materials Science & Technology* **44**, 116.
- [4] M. Mézard and A. Montanari, *Information, physics, and computation*, Oxford graduate texts (Oxford university press).
- [5] C. A. Floudas and P. M. Pardalos, eds., *Encyclopedia of Optimization*, 2nd ed. (Springer).
- [6] A. Lucas, Ising formulations of many NP problems, *Frontiers in Physics* **2**.
- [7] A. Mott, J. Job, J.-R. Vlimant, D. Lidar, and M. Spiropulu, Solving a higgs optimization problem with quantum annealing for machine learning, *Nature* **550**, 375, ADS Bibcode: 2017Natur.550..375M.
- [8] A. D. King, C. D. Batista, J. Raymond, T. Lanting, I. Ozfidan, G. Poulin-Lamarre, H. Zhang, and M. H. Amin, Quantum annealing simulation of out-of-equilibrium magnetization in a spin-chain compound, *PRX Quantum* **2**, 030317 (), ADS Bibcode: 2021PRXQ...2c0317K.
- [9] S. Abel and M. Spannowsky, Quantum-field-theoretic simulation platform for observing the fate of the false vacuum, *PRX Quantum* **2**, 010349, publisher: American Physical Society.
- [10] N. Mohseni, P. L. McMahon, and T. Byrnes, Ising machines as hardware solvers of combinatorial optimization problems, *Nature Reviews Physics* **4**, 363, ADS Bibcode: 2022NatRP...4..363M.
- [11] M. Mezard, G. Parisi, and M. A. Virasoro, *SPIN GLASS THEORY AND BEYOND: AN INTRODUCTION TO THE REPLICIA METHOD AND ITS APPLICATIONS* (World Scientific Publishing Company).
- [12] A. Perdomo-Ortiz, N. Dickson, M. Drew-Brook, G. Rose, and A. Aspuru-Guzik, Finding low-energy conformations of lattice protein models by quantum annealing, *Scientific Reports* **2**, 571, ADS Bibcode: 2012NatSR...2E.571P.
- [13] R. Dridi and H. Alghassi, Prime factorization using quantum annealing and computational algebraic geometry, *Scientific Reports* **7**, 43048.
- [14] S. Jiang, K. A. Brittt, A. J. McCaskey, T. S. Humble, and S. Kais, Quantum annealing for prime factorization, *Scientific Reports* **8**, 17667.
- [15] J. C. Criado and M. Spannowsky, Qade: Solving differential equations on quantum annealers, 2204.03657.
- [16] F. Phillipson and H. S. Bhatia, Portfolio optimisation using the d-wave quantum annealer, in *Computational Science – ICCS 2021*, edited by M. Paszynski, D. Kranzlmüller, V. V. Krzhizhanovskaya, J. J. Dongarra, and P. M. A. Sloot (Springer International Publishing) pp. 45–59.
- [17] S. F. Edwards and P. W. Anderson, Theory of spin glasses, *Journal of Physics F Metal Physics* **5**, 965, ADS Bibcode: 1975JPhF...5..965E.
- [18] D. Sherrington and S. Kirkpatrick, Solvable model of a spin-glass, *Physical Review Letters* **35**, 1792, publisher: American Physical Society.
- [19] K. Binder and A. P. Young, Spin glasses: Experimental facts, theoretical concepts, and open questions, *Reviews of Modern Physics* **58**, 801, ADS Bibcode: 1986RvMP...58..801B.
- [20] A. P. Young, Spin glasses: a computational challenge for the 21st century, *Computer Physics Communications Proceedings of the STATPHYS Satellite Conference: Challenges in Computational Statistical Physics in the 21st Century*, **146**, 107.
- [21] S. Boettcher, Physics of the edwards–anderson spin glass in dimensions  $d = 3, \dots, 8$  from heuristic ground state optimization, *Frontiers in Physics* **12**, 10.3389/fphy.2024.1466987, publisher: Frontiers.
- [22] S. Istrail, Statistical mechanics, three-dimensionality and NP-completeness: I. universality of intracatability for the partition function of the ising model across non-planar surfaces (extended abstract), in *Proceedings of the thirty-second annual ACM symposium on Theory of computing, STOC '00* (Association for Computing Machinery) pp. 87–96.
- [23] A. K. Hartmann, Ground states of two-dimensional ising spin glasses: Fast algorithms, recent developments and a ferromagnet-spin glass mixture, *Journal of Statistical Physics* **144**, 519.
- [24] M. R. Garey and D. S. Johnson, *Computers and Intractability: A Guide to the Theory of NP-Completeness*, first edition ed. (W. H. Freeman).
- [25] S. Arora and B. Barak, *Computational Complexity: A Modern Approach*, 1st ed. (Cambridge University Press).
- [26] W. K. Hastings, Monte carlo sampling methods using markov chains and their applications, *Biometrika* **57**, 97, ADS Bibcode: 1970Bimka..57...97H.
- [27] R. P. Feynman, Simulating physics with computers, *International Journal of Theoretical Physics* **21**, 467.
- [28] S. Kirkpatrick, C. D. Gelatt, and M. P. Vecchi, Optimization by simulated annealing, *Science* **220**, 671, ADS

- Bibcode: 1983Sci...220..671K.
- [29] A. B. Finnila, M. A. Gomez, C. Sebenik, C. Stenson, and J. D. Doll, Quantum annealing: A new method for minimizing multidimensional functions, *Chemical Physics Letters* **219**, 343, ADS Bibcode: 1994CPL...219..343F.
- [30] K. Hukushima and K. Nemoto, Exchange monte carlo method and application to spin glass simulations, *Journal of the Physical Society of Japan* **65**, 1604, publisher: The Physical Society of Japan.
- [31] T. Kadowaki and H. Nishimori, Quantum annealing in the transverse ising model, *Physical Review E* **58**, 5355, ADS Bibcode: 1998PhRvE..58.5355K.
- [32] J. Brooke, D. Bitko, T. F. Rosenbaum, and G. Aeppli, Quantum annealing of a disordered magnet, *Science* **284**, 779, ADS Bibcode: 1999Sci...284..779B.
- [33] J. Houdayer and O. C. Martin, Renormalization for discrete optimization, *Physical Review Letters* **83**, 1030, publisher: American Physical Society.
- [34] E. Farhi, J. Goldstone, S. Gutmann, and M. Sipser, Quantum computation by adiabatic evolution, arXiv e-prints, quant (), ADS Bibcode: 2000quant.ph..1106F.
- [35] E. Farhi, J. Goldstone, S. Gutmann, J. Lapan, A. Lundgren, and D. Preda, A quantum adiabatic evolution algorithm applied to random instances of an NP-complete problem, *Science* **292**, 472 (), publisher: American Association for the Advancement of Science.
- [36] G. E. Santoro, R. Martoňák, E. Tosatti, and R. Car, Theory of quantum annealing of an ising spin glass, *Science* **295**, 2427, ADS Bibcode: 2002Sci...295.2427S.
- [37] D. J. Earl and M. W. Deem, Parallel tempering: Theory, applications, and new perspectives, *Physical Chemistry Chemical Physics (Incorporating Faraday Transactions)* **7**, 3910, ADS Bibcode: 2005PCCP...7.3910E.
- [38] G. E. Santoro and E. Tosatti, TOPICAL REVIEW: Optimization using quantum mechanics: quantum annealing through adiabatic evolution, *Journal of Physics A Mathematical General* **39**, R393, ADS Bibcode: 2006JPhA...39R.393S.
- [39] A. Das and B. K. Chakrabarti, Colloquium: Quantum annealing and analog quantum computation, *Reviews of Modern Physics* **80**, 1061, publisher: American Physical Society.
- [40] S. Morita and H. Nishimori, Mathematical foundation of quantum annealing, *Journal of Mathematical Physics* **49**, 125210, ADS Bibcode: 2008JMP...49I5210M.
- [41] E. Farhi, J. Goldstone, and S. Gutmann, A quantum approximate optimization algorithm (), 1411.4028.
- [42] Z. Zhu, A. J. Ochoa, and H. G. Katzgraber, Efficient cluster algorithm for spin glasses in any space dimension, *Physical Review Letters* **115**, 077201, publisher: American Physical Society.
- [43] J. E. Dorband, A method of finding a lower energy solution to a QUBO/ising objective function, 1801.04849.
- [44] A. J. Ochoa, D. C. Jacob, S. Mandrà, and H. G. Katzgraber, Feeding the multitude: A polynomial-time algorithm to improve sampling, 1801.07681.
- [45] L. Zhou, S.-T. Wang, S. Choi, H. Pichler, and M. D. Lukin, Quantum approximate optimization algorithm: Performance, mechanism, and implementation on near-term devices, *Physical Review X* **10**, 021067, publisher: American Physical Society.
- [46] C. Fan, M. Shen, Z. Nussinov, Z. Liu, Y. Sun, and Y.-Y. Liu, Searching for spin glass ground states through deep reinforcement learning, *Nature Communications* **14**, 725, publisher: Nature Publishing Group.
- [47] A. Misra-Spieldenner, T. Bode, P. K. Schuhmacher, T. Stollenwerk, D. Bagrets, and F. K. Wilhelm, Mean-field approximate optimization algorithm, *PRX Quantum* **4**, 030335, publisher: American Physical Society.
- [48] H. M. Bauza and D. A. Lidar, Scaling advantage in approximate optimization with quantum annealing, 2401.07184 [cond-mat, physics:quant-ph].
- [49] M. W. Johnson, M. H. S. Amin, S. Gildert, T. Lanting, F. Hamze, N. Dickson, R. Harris, A. J. Berkley, J. Johansson, P. Bunyk, E. M. Chapple, C. Enderud, J. P. Hilton, K. Karimi, E. Ladizinsky, N. Ladizinsky, T. Oh, I. Perminov, C. Rich, M. C. Thom, E. Tolkacheva, C. J. S. Truncik, S. Uchaikin, J. Wang, B. Wilson, and G. Rose, Quantum annealing with manufactured spins, *Nature* **473**, 194, number: 7346 Publisher: Nature Publishing Group.
- [50] N. G. Dickson, M. W. Johnson, M. H. Amin, R. Harris, F. Altomare, A. J. Berkley, P. Bunyk, J. Cai, E. M. Chapple, P. Chavez, F. Cioata, T. Cirip, P. Debuen, M. Drew-Brook, C. Enderud, S. Gildert, F. Hamze, J. P. Hilton, E. Hoskinson, K. Karimi, E. Ladizinsky, N. Ladizinsky, T. Lanting, T. Mahon, R. Neufeld, T. Oh, I. Perminov, C. Petroff, A. Przybysz, C. Rich, P. Spear, A. Tcaciuc, M. C. Thom, E. Tolkacheva, S. Uchaikin, J. Wang, A. B. Wilson, Z. Merali, and G. Rose, Thermally assisted quantum annealing of a 16-qubit problem, *Nature Communications* **4**, 1903, ADS Bibcode: 2013NatCo...4.1903D.
- [51] M. Ohkuwa, H. Nishimori, and D. A. Lidar, Reverse annealing for the fully connected  $\mathbb{S}^p$ -spin model, *Physical Review A* **98**, 022314, publisher: American Physical Society.
- [52] Y. Yamashiro, M. Ohkuwa, H. Nishimori, and D. A. Lidar, Dynamics of reverse annealing for the fully connected  $\mathbb{S}^p$ -spin model, *Physical Review A* **100**, 052321, publisher: American Physical Society.
- [53] C. Cao, J. Xue, N. Shannon, and R. Joynt, Speedup of the quantum adiabatic algorithm using delocalization catalysis, *Physical Review Research* **3**, 013092.
- [54] A. D. King, S. Suzuki, J. Raymond, A. Zucca, T. Lanting, F. Altomare, A. J. Berkley, S. Ejtemaee, E. Hoskinson, S. Huang, E. Ladizinsky, A. J. R. MacDonald, G. Marsden, T. Oh, G. Poulin-Lamarre, M. Reis, C. Rich, Y. Sato, J. D. Whittaker, J. Yao, R. Harris, D. A. Lidar, H. Nishimori, and M. H. Amin, Coherent quantum annealing in a programmable 2,000 qubit ising chain, *Nature Physics* **18**, 1324 (), number: 11 Publisher: Nature Publishing Group.
- [55] A. D. King, J. Raymond, T. Lanting, R. Harris, A. Zucca, F. Altomare, A. J. Berkley, K. Boothby, S. Ejtemaee, C. Enderud, E. Hoskinson, S. Huang, E. Ladizinsky, A. J. R. MacDonald, G. Marsden, R. Molavi, T. Oh, G. Poulin-Lamarre, M. Reis, C. Rich, Y. Sato, N. Tsai, M. Volkmann, J. D. Whittaker, J. Yao, A. W. Sandvik, and M. H. Amin, Quantum critical dynamics in a 5000-qubit programmable spin glass, *Nature* 10.1038/s41586-023-05867-2 (), 2207.13800 [cond-mat, physics:quant-ph].
- [56] M. Bernaschi, I. González-Adalid Pemartín, V. Martín-Mayor, and G. Parisi, The quantum transition of the two-dimensional ising spin glass, *Nature* **631**, 749, publisher: Nature Publishing Group.
- [57] M. Palassini, F. Liers, M. Juenger, and A. P. Young, Low-energy excitations in spin glasses from exact ground states, *Physical Review B* **68**, 064413.



- [58] A. Montanaro, Quantum speedup of branch-and-bound algorithms, *Physical Review Research* **2**, 013056, publisher: American Physical Society.
- [59] W. L. McMillan, Scaling theory of ising spin glasses, *Journal of Physics C: Solid State Physics* **17**, 3179.
- [60] D. S. Fisher and D. A. Huse, Ordered phase of short-range ising spin-glasses, *Physical Review Letters* **56**, 1601, publisher: American Physical Society.
- [61] M. A. Moore, H. Bokil, and B. Drossel, Evidence for the droplet picture of spin glasses, *Physical Review Letters* **81**, 4252, publisher: American Physical Society.
- [62] M. Palassini and A. P. Young, Nature of the spin glass state, *Physical Review Letters* **85**, 3017, cond-mat/0002134.
- [63] E. Marinari and G. Parisi, Effects of changing the boundary conditions on the ground state of ising spin glasses, *Physical Review B* **62**, 11677 ().
- [64] S. Franz and G. Parisi, Non trivial overlap distributions at zero temperature, *The European Physical Journal B* **18**, 485.
- [65] E. Marinari and G. Parisi, Effects of a bulk perturbation on the ground state of 3d ising spin glasses, *Physical Review Letters* **86**, 3887 ().
- [66] C. M. Newman and D. L. Stein, Finite-dimensional spin glasses: States, excitations, and interfaces, *Annales Henri Poincaré* **4**, 497.
- [67] J. Collaboration, R. A. Banos, A. Cruz, L. A. Fernandez, J. M. Gil-Narvion, A. Gordillo-Guerrero, M. Guidetti, A. Maiorano, F. Mantovani, E. Marinari, V. Martin-Mayor, J. Monforte-Garcia, A. M. Sudupe, D. Navarro, G. Parisi, S. Perez-Gavero, J. J. Ruiz-Lorenzo, S. F. Schifano, B. Seoane, A. Tarancon, R. Tripiccion, and D. Yllanes, Nature of the spin-glass phase at experimental length scales, *Journal of Statistical Mechanics: Theory and Experiment* **2010**, P06026, 1003.2569 [cond-mat].
- [68] G. Parisi and T. Temesvári, Replica symmetry breaking in and around six dimensions, *Nuclear Physics B* **858**, 293.
- [69] M. A. Moore, Droplet-scaling versus replica symmetry breaking debate in spin glasses revisited, *Physical Review E* **103**, 062111, publisher: American Physical Society.
- [70] M. Shen, G. Ortiz, Y.-Y. Liu, M. Weigel, and Z. Nussinov, Universal fragility of spin glass ground states under single bond changes, *Physical Review Letters* **132**, 247101.
- [71] J. Houdayer, F. Krzakala, and O. Martin, Large-scale low-energy excitations in 3-d spin glasses, *The European Physical Journal B - Condensed Matter and Complex Systems* **18**, 467.
- [72] F. Krzakala and O. C. Martin, Spin and link overlaps in three-dimensional spin glasses, *Physical Review Letters* **85**, 3013, publisher: American Physical Society.
- [73] H. Wang, H.-C. Yeh, and A. Kamenev, Many-body localization enables iterative quantum optimization, *Nature Communications* **13**, 5503, number: 1 Publisher: Nature Publishing Group.
- [74] H. Zhang, K. Boothby, and A. Kamenev, Cyclic quantum annealing: searching for deep low-energy states in 5000-qubit spin glass, *Scientific Reports* **14**, 30784, publisher: Nature Publishing Group.
- [75] One may worry about using the notion of temperature for the intrinsically non-equilibrium glassy system. Indeed, an evolution is non-ergodic and is getting stuck in a local minimum. We use the cyclic annealing with random initial conditions to generate a large ensemble of such local minima which mimics ergodicity. In the end, the effective temperature is only a proxy for the excess energy per spin in such an ensemble.
- [76] While the adiabatic quantum annealing is, in principle, capable of reaching an exact ground state (also in probabilistic sense), its efficiency is fundamentally limited to  $\beta \approx 1$ , due to exponentially small energy gaps along the annealing path and non-adiabatic Landau-Zener transitions across them.
- [77] For example, the cyclic annealing achieves a lower effective temperature than the forward annealing [74].
- [78] K. Boothby, P. Bunyk, J. Raymond, and A. Roy, Next-generation topology of d-wave quantum processors, 2003.00133 [quant-ph].
- [79] P. Virtanen, R. Gommers, T. E. Oliphant, M. Haberland, T. Reddy, D. Cournapeau, E. Burovski, P. Peterson, W. Weckesser, J. Bright, S. J. van der Walt, M. Brett, J. Wilson, K. J. Millman, N. Mayorov, A. R. J. Nelson, E. Jones, R. Kern, E. Larson, C. J. Carey, Í. Polat, Y. Feng, E. W. Moore, J. VanderPlas, D. Laxalde, J. Perktold, R. Cimrman, I. Henriksen, E. A. Quintero, C. R. Harris, A. M. Archibald, A. H. Ribeiro, F. Pedregosa, P. van Mulbregt, and SciPy 1.0 Contributors, SciPy 1.0: Fundamental Algorithms for Scientific Computing in Python, *Nature Methods* **17**, 261 (2020).
- [80] Hereafter, we use the reduced Hamming distance, defined as  $d = \min(\tilde{d}, N - \tilde{d})$ , where  $\tilde{d}$  is the original definition of Hamming distance, since flipping all spins yields an equivalent state with identical energy.
- [81] We are indebted to Michael Winer for discussion of this issue.
- [82] A. Montanaro, Quantum speedup of branch-and-bound algorithms, *Physical Review Research* **2**, 013056 (2020), arXiv:1906.10375 [cs.DS].
- [83] A. Misra-Spieldenner, T. Bode, P. K. Schuhmacher, T. Stollenwerk, D. Bagrets, and F. K. Wilhelm, Mean-field approximate optimization algorithm, *PRX Quantum* **4**, 030335 (2023).
- [84] H. Schlömer and S. Sachdev, Quantum annealing with chaotic driver hamiltonians, 2409.20538.